



**HAL**  
open science

## Phenolic substrates and suicide inactivation of tyrosinase: kinetics and mechanism

Jose Luis Muñoz-Muñoz, Francisco Garcia-Molina, Pedro Antonio Garcia-Ruiz, Milagros Molina-Alarcon, Jose Tudela, Francisco Garcia-Canovas, Jose Neptuno Rodriguez-Lopez

### ► To cite this version:

Jose Luis Muñoz-Muñoz, Francisco Garcia-Molina, Pedro Antonio Garcia-Ruiz, Milagros Molina-Alarcon, Jose Tudela, et al.. Phenolic substrates and suicide inactivation of tyrosinase: kinetics and mechanism. *Biochemical Journal*, 2008, 416 (3), pp.431-440. 10.1042/BJ20080892 . hal-00479021

**HAL Id: hal-00479021**

**<https://hal.science/hal-00479021>**

Submitted on 30 Apr 2010

**HAL** is a multi-disciplinary open access archive for the deposit and dissemination of scientific research documents, whether they are published or not. The documents may come from teaching and research institutions in France or abroad, or from public or private research centers.

L'archive ouverte pluridisciplinaire **HAL**, est destinée au dépôt et à la diffusion de documents scientifiques de niveau recherche, publiés ou non, émanant des établissements d'enseignement et de recherche français ou étrangers, des laboratoires publics ou privés.

Running title: Mechanism of suicide inactivation of tyrosinase

## Phenolic substrates and suicide inactivation of tyrosinase: kinetics and mechanism.

### AUTHORS

Muñoz-Muñoz, J.L.<sup>1</sup>, García-Molina, F.<sup>1</sup>, García-Ruiz, P.A.<sup>2</sup>, Molina-Alarcón, M.<sup>3</sup>, Tudela, J.<sup>1</sup>, García-Cánovas, F.<sup>1\*</sup>, and Rodríguez-López, J.N.<sup>1</sup>.

### ADRESSES

<sup>1</sup>GENZ: Grupo de Investigación de Enzimología, Departamento de Bioquímica y Biología Molecular-A, Facultad de Química, Universidad de Murcia, E-30100 Espinardo, Murcia, Spain.

<sup>2</sup>QCBA: Grupo de Química de Carbohidratos y Biotecnología de Alimentos, Departamento de Química Orgánica. Facultad de Química, Universidad de Murcia, E-30100 Espinardo, Murcia, Spain.

<sup>3</sup>Departamento de Enfermería, Escuela Universitaria de Enfermería, Universidad de Castilla la Mancha, E-02071, Albacete, Spain.

\*Corresponding author. Fax: +34 968 363963

E-mail: [canovasf@um.es](mailto:canovasf@um.es), <http://www.um.es/genz>.

## ABSTRACT

The suicide inactivation mechanism of tyrosinase acting on its substrates has been studied. The kinetic analysis of the proposed mechanism during the transition phase provides explicit analytical expressions for the concentrations of *o*-quinone *versus* time. The electronic, steric and hydrophobic effects of the substrates influence the enzymatic reaction, increasing the catalytic speed by three orders of magnitude and the inactivation by one order of magnitude. To explain the suicide inactivation, we propose a mechanism, in which the enzymatic form  $E_{ox}$  is responsible for such inactivation. A key step might be the transfer of the C-1 hydroxyl group proton to the peroxide, which would act as a general base. Another essential step might be the axial attack of the *o*-diphenol on the copper atom. The rate constant of this reaction would be directly related with the strength of the nucleophilic attack of the C-1 hydroxyl group, which depends on the chemical shift of the carbon C-1 ( $\delta_1$ ) obtained by  $^{13}\text{C}$ -NMR. Protonation of the peroxide would bring the copper atoms together and encourage the diaxial nucleophilic attack of the C-2 hydroxyl group, facilitating the co-planarity with the ring of the copper atoms and the concerted oxidation/reduction reaction, and giving rise to an *o*-quinone. The suicide inactivation would occur if the C-2 hydroxyl group transferred the proton to the protonated peroxide, which would again act as a general base. In this case, the co-planarity between the copper atom, the oxygen of the C-1 and the ring would only permit the oxidation/reduction reaction on one copper atom, giving rise to copper (0), hydrogen peroxide and an *o*-quinone, which would be released, thus inactivating the enzyme.

Keywords: mechanism-based inhibitors, mushroom tyrosinase, suicide inactivation, deprotonation, diaxial, equatorial.

## INTRODUCTION

Tyrosinase or polyphenol oxidase (EC 1.14.18.1) is a copper protein that uses molecular oxygen to catalyse the hydroxylation of monophenols to *o*-diphenols (monophenolase activity) and the oxidation of *o*-diphenols to *o*-quinones (diphenolase activity) [1,2]. Tyrosinase undergoes an inactivation process when it reacts with its substrate, a phenomenon that has long been known in the case of enzymes from a variety of natural sources, including fungi, plants and animals [3-9]. The study of enzymatic inactivation by suicide substrates or mechanism-based inhibitors is of growing importance because of possible pharmacological applications [10,11]. In the case of mammalian, viral, bacterial or parasitic proteases, a recent review looked at the design of mechanism-based enzyme inhibitors [10]. In addition, suicide substrates and mechanism-based enzyme inactivators may be useful for studying enzymatic mechanisms and designing of new drugs [12]. Since tyrosinase participates in different physiological processes, such as fruit and vegetable browning and pigmentation in animals [2], the suicide inactivation of this enzyme is of even more interest.

We have made several kinetic studies of suicide inactivation mechanisms using mushroom tyrosinase [13], frog skin tyrosinase [14,15] and peroxidase from different sources [16,17]. We have also studied the suicide inactivation of an enzyme that can be measured from coupled reactions [18] and published a totally experimental study which used several experimental designs to kinetically study suicide inactivation [19].

The kinetics of the suicide inactivation of tyrosinase have been studied and characterised by determining the kinetic parameters that identify a suicide substrate:  $\lambda_{\max}$  (maximum apparent inactivation constant), partition ratio between the catalytic and the inactivation pathways "*r*" and the Michaelis constant  $K_m^S$ . However, the molecular processes that lead to the suicide inactivation of tyrosinase have not been

fully clarified [13-15,18]. To date, three mechanisms have been proposed to explain this inactivation: (i) an attack by the *o*-quinone product on a sensitive nucleophilic group vicinal to the active site [5], (ii) free radical attack on the active site by the reactive oxygen species (ROS) generated during the catalytic oxidation [7] and (iii) a mechanism that involves catechol substrate presenting itself at the active site as a cresol, "cresolase presentation". This leads to the catechol being oxidised to form a product able to undergo deprotonation and reductive elimination, resulting in inactivation of the enzyme through the formation of copper (0) at the active site [20].

With regard to the first two mechanisms proposed, in experiments where *o*-quinone binding was prevented, there was no influence on inactivation, and attempts to protect the enzyme with radical scavengers proved unsuccessful [8,21]. As regards the third mechanism, the presentation of the *o*-diphenol as a monophenol (cresolase presentation) [20], the firmest evidence to support this, according to the authors, is the fact that trihydroxylated compounds such as pyrogallol do not produce inactivation.

In recent years we have taken a closer look at the tyrosinase catalysis mechanism, both as regards its monophenolase and diphenolase activities [1,22-27], and proposed a structural mechanism to explain the enzyme behaviour [28]. We have also studied the kinetics of the lag phase in monophenolase activity [29], although the structural mechanism of the suicide mechanism has been overlooked. To our mind, the study most directly related with suicide inactivation was one that considered the hydroxylation of monophenols to *o*-diphenols, whereby it was proposed that from the (enzyme-diphenol) complex generated, the *o*-diphenol may be oxidised to *o*-quinone, or be released to the medium as *o*-diphenol [28]. In this way, when oxy-tyrosinase ( $E_{ox}$ ) binds to the monophenol, it is hydroxylated in the ortho position so that it remains in an axial-equatorial position. From this position, the enzyme releases the *o*-diphenol

generated from the equatorial position, breaking the axial bond and giving rise to *met*-tyrosinase ( $E_m$ ) + *o*-diphenol, or re-binding the *o*-diphenol in diaxial position and oxidising it, giving rise to *deoxy*-tyrosinase ( $E_d$ ) + *o*-quinone. Hence, an explanation for the suicide inactivation (Scheme I) would be that the binding of  $E_{ox}$  to the *o*-diphenol involves two possible alternatives: a) diaxial binding with the copper atoms through the hydroxyl groups of C-1 and C-2, leading to the concerted oxidation/reduction of the *o*-diphenol to  $E_m$  + *o*-quinone (catalytic pathway), or b) axial binding with one copper atom through the hydroxyl group of C-1, while the hydroxyl group of C-2 transfers its proton to the peroxide. In the latter case, the concerted oxidation/reduction step could not occur, due to the lack of co-planarity. However, oxidation/reduction on one atom of copper could occur, the copper passing to copper (0) and forming *o*-quinone, hydrogen peroxide and inactive enzyme (inactivation pathway). We attempt to confirm this hypothesis (Scheme I) by experimental data, which can be correlated with the hydrophobic, steric and electronic effects. These effects are related with the catalysis and inactivation capacity of the enzyme by their substrates.

**ABBREVIATIONS**

For clarity and for the sake of brevity, the following abbreviations will be used in the text.

**Species and concentrations**

$E_m$	<i>met</i> -tyrosinase.
$E_d$	<i>deoxy</i> -tyrosinase.
$E_{ox}$	<i>oxy</i> -tyrosinase.
$E_i$	inactive enzyme.
$[E]_0$	initial concentration of tyrosinase.
$S$	<i>o</i> -diphenol acting as suicide substrate.
$[S]_0$	initial concentration of <i>o</i> -diphenol substrate.
$[O_2]$	instantaneous concentration of oxygen.
$[O_2]_0$	initial concentration of oxygen.
$Q$	product of the enzymatic reaction.
$[Q]$	instantaneous concentration of $Q$ .

**Kinetic parameters**

$\lambda$	apparent inactivation constant.
$[Q]_\infty$	concentration of product $Q$ obtained at end of the reaction.
$[O_2]_f$	oxygen remaining at $t \rightarrow \infty$ .
$[O_2]_\infty$	oxygen consumed at $t \rightarrow \infty$ . $[O_2]_\infty = [O_2]_0 - [O_2]_f$ .
$V_0$	initial rate of the catalytic pathway.
$k_x$	rate constants of the catalytic pathway.
$k_x^i$	rate constants of the inactivation pathway.
$r$	partition ratio $r = k_{7_2} / k_{7_2}^i = k_{cat} / \lambda_{max}$ .

$K_m^{O_2}$	Michaelis constant for oxygen.
$K_m^S$	Michaelis constant of tyrosinase for $S$ .
$k_{cat}$	catalytic constant of the catalytic pathway ( $k_{cat} = \lambda_{max} r$ ).
$\lambda_{max}$	maximum value of $\lambda$ for saturating $S$ .

Stage 2(a) POST-PRINT

## MATERIAL AND METHODS

### Reagents

Mushroom tyrosinase or polyphenol oxidase (*o*-diphenol: $O_2$  oxidoreductase, EC 1.14.18.1, 8300 units/mg) and  $\beta$ -NADH were supplied by Sigma. The enzyme was purified as previously described in [25]. The substrates used were: pyrogallol, catechol, 4-chlorocatechol, 4-methylcatechol, 4-ethylcatechol, 4-*tert*-butylcatechol, 3,4-dihydroxyphenylpropionic acid (DHPPA), 3,4-dihydroxyphenylacetic acid (DHPAA), gallic acid methyl ester, gallic acid, protocatechuic acid, protocatechuic aldehyde and 4-nitrocatechol (all from Sigma). The corresponding structures are shown in Table 1. Other chemicals were of analytical grade.

The kinetic assays to study suicide inactivation use spectrophotometric and oxymetric methods [30,31].

### Spectrophotometric assays

These assays were carried out with a Perkin-Elmer Lambda-35 spectrophotometer, on line interfaced to a PC-computer, where the kinetic data were recorded, stored and later analyzed. The product of the enzyme reaction, the *o*-quinone, is not suitable for experimental detection at long assay times due to the instability of the *o*-quinones [32,33]. Depending on the spectrum of the substrate and oxidation potential of the corresponding *o*-quinone, the reaction was followed by measuring: (a) the disappearance of NADH at 340 nm, with  $\epsilon = 6230 \text{ M}^{-1} \text{ cm}^{-1}$  (4-chlorocatechol, 4-methylcatechol, 4-ethylcatechol, 4-nitrocatechol, DHPPA, DHPAA, catechol, 4-*tert*-butyl-catechol, protocatechuic acid and protocatechuic aldehyde) or b) the disappearance of ascorbic acid at 290 nm with  $\epsilon = 2175 \text{ M}^{-1} \text{ cm}^{-1}$  (pyrogallol) [34].

### Oxymetric assays

When the substrate and NADH (or ascorbic acid) spectra overlapped, oxymetric assays were carried out [31]. Measurements of dissolved oxygen concentration were made with a Hansatech (Kings Lynn, Cambs, U.K.) oxygraph unit controlled by a PC. The oxygraph used a Clark-type silver/platinum electrode with a 12.5  $\mu\text{m}$  Teflon membrane. The sample was continuously stirred during the experiments and its temperature was maintained at 25  $^{\circ}\text{C}$ . The zero oxygen level for calibration and the experiments was obtained by bubbling oxygen-free nitrogen through the sample for at least 10 min. The substrates gallic acid and gallic acid methyl ester were studied by means of this method.

The effects of various reagents were studied. Their concentrations are given in detail in the corresponding figures of the Results section. In all assays, the following reagents were maintained constant: 0.26 mM  $O_2$  (saturating), 30 mM phosphate buffer pH 7.0,  $AH_2$  or  $NADH$ . Protein concentration was determined by the Lowry method [35].

### Data analysis

The experimental data for the disappearance of  $NADH$  or  $AH_2$  with time (Fig. 1) follow the equation:

$$[NADH] = [NADH]_0 - [Q] = [NADH]_0 - [c_1(1 - e^{-c_2t}) + c_3 + c_4t] \quad (1)$$

or

$$[AH_2] = [AH_2]_0 - [Q] = [AH_2]_0 - [c_1(1 - e^{-c_2t}) + c_3 + c_4t] \quad (2)$$

in which  $c_i$  ( $i = 1 - 4$ ) can be obtained by non-linear regression [36].

The parameter  $c_1$  is equal to  $[Q]_\infty$  and  $c_2$  to the corresponding  $\lambda$ . The coefficient  $c_3$  represents the uncertainty at zero time absorbance caused by addition of the enzyme at the start of the reaction, while  $c_4$  corresponds to the slow spontaneous oxidation of *o*-diphenol and *NADH* or *AH<sub>2</sub>*. The effects of both experimental artefacts (Fig. 1) should be computer subtracted in further *NADH* vs. time or *AH<sub>2</sub>* vs. time plots. The experimental recording obtained in the following steps therefore fit Equation 1 or 2, from which the corresponding inactivation parameters,  $[Q]_\infty$  and  $\lambda$ , can be determined.

When the disappearance of oxygen is measured:

$$[O_2] = [O_2]_0 - [c_1(1 - e^{-c_2 t}) + c_3 + c_4 t] = [O_2]_f + [O_2]_\infty e^{-\lambda t} - c_4 t \quad (3)$$

Note that  $[O_2]_\infty$  ( $c_1 = c_1/2$ ) becomes  $[Q]_\infty/2$ , reflecting the stoichiometry of the reaction (Scheme II), and the spontaneous oxidation rate of the substrate is represented by  $c_4$ .

### Kinetic characteristics of the oxidation of trihydroxylated substrates

In the case of vicinal trihydroxylated phenolic substrates, the kinetic assays should be carried out in the presence of superoxide dismutase (SOD), since the spontaneous oxidation of these compounds is very strong and superoxide anion is formed, generating an autocatalytic oxidation mechanism. In the presence of SOD, however, this mechanism is inhibited and the inactivation kinetics can be followed spectrophotometrically or oxymetrically.

### <sup>13</sup>C-NMR

For all the substrates used, the <sup>13</sup>C-NMR spectra were obtained in deuterated water pH 7.0, which provided the shifts of the C-1 ( $\delta_1^7$ ) and C-2 ( $\delta_2^7$ ) carbons for the different *o*-diphenols. The <sup>13</sup>C-NMR spectra of the different *o*-diphenols considered here were obtained in a 300 MHz Varian Unity spectrometer. The  $\delta$  values were measured relative to those for tetramethylsilane ( $\delta=0$ ). The maximum line breadth accepted in the <sup>13</sup>C-NMR spectra was 0.06 Hz. Therefore, the maximum accepted error for each peak was  $\pm 0.03$  p.p.m. Moreover, the electron-donating capacity of the oxygen atom from different phenolic compounds (nucleophilic power) was correlated with the experimental  $\delta$  values in <sup>13</sup>C-NMR for the carbon atom that supports the hydroxyl group. Taking all the above into account, low values of  $\delta_1^7$  and  $\delta_2^7$  in <sup>13</sup>C-NMR for *o*-diphenols indicate high nucleophilic power at pH 7.0 [22].



$$[Q] = [Q]_{\infty}(1 - e^{-\lambda t}) = \frac{V_0}{\lambda}(1 - e^{-\lambda t}) = \frac{V_{\max}}{\lambda_{\max}}(1 - e^{-\lambda t}) \quad (4)$$

when  $t \rightarrow \infty$ , results:

$$[Q]_{\infty} = \frac{2k_{cat}}{\lambda_{\max}}[E]_0 = \frac{2k_{7_2}}{k_{7_2}^i}[E]_0 = 2r[E]_0 \quad (5)$$

Bearing in mind that  $K_m^{O_2}$  values are very low [37] and that the initial oxygen concentration is 0.26 mM, the enzyme is saturated with  $O_2$  and, from Equations S8 and S9, we obtain:

$$\lambda = \frac{\lambda_{\max}[S]_0}{K_m^S + [S]_0} \quad (6)$$

and

$$V_0 = \frac{2k_{cat}[S]_0[E]_0}{K_m^S + [S]_0} \quad (7)$$

### Experimental design

The experimental study of the kinetics of suicide substrates or mechanism-based enzyme inhibitors is important for obtaining reliable kinetic parameters ( $\lambda_{\max}$ ,  $K_m^S$  and  $r$ ) that will permit any *in vitro* information gained to be extrapolated to *in vivo* situations [11]. A recent revision of the inactivation of cytochromes P450 (CYPs) by metabolic products that form heme or protein adducts or a metabolic inhibitory complex, known as mechanism-based enzyme inhibitors, underlined the importance of kinetic studies, always making discontinuous measurements (preincubating the enzyme with the suicide substrate and taking aliquots to follow the diminution of enzymatic activity with time) [11].

In a previous study, we outlined the methodology necessary for kinetically characterising a suicide substrate following the reaction continuously [19]. Two basic situations were described: a) the suicide substrate gives rise to an easily measurable product, in which case the kinetics is studied by measuring this product, or b) when the suicide substrate gives rise to a product that cannot be measured easily, in which case a non-suicide auxiliary substrate is necessary to characterise the inactivation kinetics continuously. In the present work, we apply the experimental design described in [19] to the suicide inactivation of tyrosinase as it acts on *o*-diphenols since, although the products obtained, *o*-quinones, are unstable [32,33], they can be reduced by *NADH* or *AH<sub>2</sub>* and the disappearance of these coupled reagents can be measured. Alternatively, the consumption of oxygen can be measured in an oxygraph since oxygen is also a substrate of the enzyme. The experimental design can be described in three stages:

Step 1: Preliminary assays, in which the experimental conditions are optimised and the design is detailed.

Step 2: Study of the variation in enzyme concentration and determination of the parameter *r*.

Step 3: study of the variation of substrate concentration and determination of  $\lambda_{\max}$ ,  $K_m^S$ .

### Experimental study of suicide inactivation

The following *o*-diphenols are used in this work: Catechol, 4-chlorocatechol, 4-methylcatechol, 4-ethylcatechol, 4-*tert*-butylcatechol, DHPPA, DHPAA, 4-nitrocatechol, protocatechuic acid and protocatechuic aldehyde (see Table 1).

Step 1. Fig. 1 shows the spectrophotometric recordings of the disappearance of  $AH_2$  (curves (a) and (c)) and their corrections after fitting according to Equation 2 and after subtracting the parameters  $c_3$  and  $c_4t$  (curves (b) and (d)). These corrected registers are analysed as described in the Data Analysis section. By means of these preliminary studies, the concentration of enzyme is optimised so that  $[Q]_\infty \ll [O_2]_0, [S]_0$ .

Step 2. Variation in enzyme concentration. The concentration of  $[E]_0$  is varied while the substrate concentration is kept constant. The results obtained in the presence of  $AH_2$ , in the case of a vicinal trihydroxylated substrate like pyrogallol, are shown in Fig. 2. The concentration of the substrate in these experiments does not change because the *o*-quinone is reduced by  $AH_2$ . However, the concentrations of  $O_2$ , or  $AH_2$  do change. In the case of the tyrosinase enzymatic system, there is the advantage that the  $K_m^{O_2}$  are very small [37], which permits an oxygen consumption of more than 10%. The  $AH_2$  must be in excess. The results obtained for catechol are shown in Fig. S1.

To study substrates like gallic acid methyl ester, whose suicide inactivation cannot be followed spectrophotometrically, an oxymetric method was employed, which measures the consumption of oxygen with time (Fig. S2). The Inset of Fig. S2 shows  $[O_2]_\infty$  vs.  $[E]_0$  and the independence of  $\lambda$  vs.  $[E]_0$ .

Fig. 3 shows the dependence of the values obtained for the product at the end of the reaction,  $[Q]_{\infty}$  vs.  $[E]_0$ , from whose slopes and according to Equation 5, the partition ratio  $r$  can be determined (see Table 2).

Step 3. Variation of concentration of substrate (*o*-diphenol). Having fixed a concentration of enzyme sufficient to give  $[Q]_{\infty}$  or  $[O_2]_{\infty} \ll [O_2]_0$  for the lowest substrate concentration being assayed, the concentration of substrate is varied while the concentration of  $O_2$  is kept constant at a saturating 0.26 mM. For the different types of substrate studied by the different methods, a hyperbolic dependence of the apparent inactivation constant is obtained in all cases with respect to the concentration of substrate (Fig. 4, Fig. S3 and Fig. S4).

Non-linear regression analysis of  $\lambda$  vs.  $[S]_0$  according to Equation 6, gives the values of  $\lambda_{\max}$ , the apparent maximum inactivation constant and  $K_m^S$ , the Michaelis constant of tyrosinase for the substrate being considered (Table 2). From these values and taking into consideration Equation 5, the catalytic constant,  $k_{cat}$ , can be obtained (see Table 2).

Figs. 5, Fig. S5A and Fig. S5B show the dependence of  $\lambda$  vs.  $[S]_0$  for the different substrates studied. An analysis according to Equation 6 provides the apparent maximum inactivation constants ( $\lambda_{\max}$ ) and the Michaelis constant  $K_m^S$  (Table 2).

## DISCUSSION

### Pharmacological importance of suicide substrates

The study of suicide inactivation and irreversible inhibition is important in the functional design of synthetic inactivators for therapeutic applications. For example, irreversible inactivators (insecticides) have been designed against acetylcholinesterase and suicide substrates of  $\beta$ -lactamases (clavulanic acid) that help the action of antibiotics (amoxicillin) [12,38].

The process of tyrosinase inactivation has long been studied in plants and animals [3]. Later, tyrosinase was studied in *Neurospora crassa* [9,21], mammals [6-8], mushroom [13,39,40] and frog skin [14,15]. Recently, a possible mechanism to explain the suicide inactivation of mushroom tyrosinase has been proposed [20]. Based on kinetic studies with tyrosinases from several vegetal sources [41,42] and mushroom in steady state [22,24], we proposed a structural mechanism to explain the kinetic results obtained at short times, where the suicide inactivation process is not significant in practice. Studies with mushroom tyrosinase in pre-steady-state permitted additional information to be obtained on the mechanism [25].

When an enzyme acts on a suicide substrate, the resulting transition phase permits us to look at the kinetics of the suicide inactivation process that coincides with enzymatic catalysis. When an enzyme acts on a suicide substrate, two pathways are set in action: the catalytic pathway, which gives rise to a product, and an inactivation pathway that gives rise to an inactive enzyme, the whole process taking place in a post-steady-state transition phase (the steady state is reached at  $t \rightarrow 0$  and then evolves in transition phase until the reaction stops since the enzyme is inactivated, hence the name post-steady-state).

In our previous studies [13-15], we tried to obtain explicit solutions for product vs. time, since these are more useful for data analysis and make it easier to obtain the kinetic information that characterises a suicide substrate: the partition coefficient,  $r$ ; the maximum apparent inactivation constant  $\lambda_{\max}$  and the Michaelis constant,  $K_m^S$ . In addition, information on the catalytic pathway (the catalytic constant  $k_{cat}$ ) is also obtained. A pre-requisite for obtaining these explicit solutions is that the substrate concentrations should vary little, that is, be almost constant: ( $[O]_{\infty} \ll [S]_0, [O_2]_0$ ). With tyrosinase, such experimental conditions can be achieved by working with low enzyme concentrations and using a reductant such as  $NADH$  or  $AH_2$ . These reduce the o-quinones, with a given stoichiometry, which means the concentration of reducing substrate (o-diphenol) remains constant. As regards the other substrate,  $O_2$ , we determined the  $K_m^{O_2}$  [37] and, at the concentration of oxygen in the solutions, (0.26 mM), the enzyme was saturated. These are the conditions used in the assays here described.

Another aspect to bear in mind is the spontaneous oxidation of the o-diphenol and triphenol substrates. In the case of vicinal triphenols, oxidation may become quite pronounced and can be stopped by adding SOD to the reaction medium. By following the steps of the experimental design described in Results, the kinetic information shown in Table 2 can be obtained.

From these data, the parallelism between the maximum apparent inactivation constant ( $\lambda_{\max}$ ) and the catalytic constant ( $k_{cat}$ ) can be seen (Table 2), confirming the kinetic analysis since both are related by Equation 5. In this way, the best substrates, like pyrogallol, catechol, 4-chlorocatechol, 4-methylcatechol (with hydrogen or donating group in C-4), show higher catalytic ( $k_{cat}$ ) and suicide inactivation ( $\lambda_{\max}$ ) constants,

while the worst substrates, like protocatechuic acid, protocatechuic aldehyde, 4-nitrocatechol (with electron withdrawing group in C-4), have a low  $k_{cat}$  and  $\lambda_{max}$ . Of note is the fact that the electronic, steric and hydrophobic effects on the substrate-enzyme binding and on the inactivation and catalysis processes affect the catalysis (constants around  $10^3$ ) and suicide inactivation (constants around 10) processes. Note how pyrogallol inactivates the enzyme in the same way as the *o*-diphenols; furthermore, as it is the best substrate of the enzyme (greater  $k_{cat}$ ), the  $\lambda_{max}$  is also greater (Table 2).

The parameter  $r = k_{7_2} / k_{7_2}^i$  indicates the probability that the hydroxyl group of C-2 will carry out a nucleophilic attack on the second copper ( $C_u^A$ ), transferring the proton to the histidine and taking up a diaxial position (see Scheme I), an assumption derived from the flexible feature of the residue histidine<sup>54</sup> previously proposed for *Streptomyces castaneoglobisporus* tyrosinase [43], or transferring the proton to the protonated peroxide, remaining in position C-1 and axially bound to the copper and to C-2 as  $C-O^-$ , a step favoured by the charge density of the copper atom bound to the substrate. When this has an electron-donating group in C-4, the positive charge density in the copper will be lower and the proton will be transferred to the histidine. In this way, the hydroxyl group in C-2 will be better able to carry out the nucleophilic attack on the copper and the proton will be transferred to the histidine, binding to the substrate in a diaxial position. When the substrate has a withdrawing group in C-4, the positive charge density of the copper atom will be greater, influencing the hydroxyl group of C-2 and favouring deprotonation, the proton being transferred to the protonated peroxide (see Scheme I). In addition, hydrophobic and esteric effects influence both process (catalysis and inactivation) (Table 2).

In the first case, the catalysis involves a concerted oxidation/reduction reaction, releasing *o*-quinone and  $E_m$  since the oxygens are co-planar with the two copper atoms. However, in the second case, the oxidation/reduction may take place on the one copper atom, releasing *o*-quinone, copper (0), hydrogen peroxide and inactive enzyme.

Table 2 shows the values of  $k_{cat}$ ,  $r$ ,  $\lambda_{max}$  and of the chemical shifts of the different suicide substrates obtained by  $^{13}\text{C}$ -NMR for the C-1 and C-2 carbons. The electronic, steric and hydrophobic effects are evident in the process of catalysis and inactivation. Note how the values of  $r$  decrease as the group in C-4 becomes more electron-withdrawing due to closer values of  $k_{7_2}$  and  $k_{7_2}^i$  (the lower corresponds to 4-nitrocatechol). It is important to note the high relation, in some cases, between the  $^{13}\text{C}$ -NMR data compared with the values of  $k_{cat}$  and  $\lambda_{max}$  shown in Table 2. In the case of pyrogallol, which has the lowest  $\delta_1$  value, the electron density of the oxygen atom of the hydroxyl group of C-1 is very high and has the highest  $k_{cat}$  and  $\lambda_{max}$  values. However, the value of  $r$  is also at its maximum for all the substrates studied, which can be explained by the greater influence of the value of  $\delta_1$  on  $k_{cat}$  ( $10^3$  range) than on  $\lambda_{max}$  (10 range). Furthermore, as this compound is vicinal trihydroxylated, the probability of catalysis taking place is doubled since there are two possible *o*-diphenol orientations. According to Scheme I, in the complex  $(E_{ox}-S)_1$ , with the substrate bound axially to the copper by C-1 (which has a lower positive charge density), the adjacent hydroxyl group has a greater possibility to bind to the second copper, transferring its proton to the histidine.

Catechol is a good tyrosinase substrate (in this case, there are no steric or hydrophobic effects that hinder the process) even though the values of  $\delta_1$  and  $\delta_2$  are

not good; however, since the OH groups are equivalent, the probability of catalysis and inactivation increases. The value of  $r$  is high, since, as in the previous case, the effect on  $k_{cat}$  is much higher than on  $\lambda_{max}$ , favouring the catalytic pathway. The group of substrates, 4-chlorocatechol, 4-methylcatechol and 4-ethylcatechol, with their very close  $\delta_1$  values, gives similar values of  $k_{cat}$ ,  $\lambda_{max}$  and  $r$  (although, in the case of 4-ethylcatechol steric effects exist) The effect of the donating group in C-4 is responsible for the powerful nucleophilic attack of the hydroxyl group in C-1. In the case of 4-*tert*-butylcatechol, although its  $\delta_1$  is similar to that of catechol, the size of the group in C-4, *tert*-butyl (steric effect), may cause steric hindrance, which decreases its  $k_{cat}$ ,  $\lambda_{max}$  and  $r$ . That is, the *tert*-butyl group affects both routes through steric hindrance.

As regards DHPPA and DHPAA, although their  $\delta_1$  are better than that of catechol, the effect of the negative charge of the carboxylic group decreases the  $k_{cat}$  and  $\lambda_{max}$  (decreased hydrophobicity). Gallic acid and gallic acid methyl ester are trihydroxylated compounds with low  $\delta_1$  values, although the withdrawing effect of the carboxyl group means that their  $k_{cat}$  and  $\lambda_{max}$  are low, as is their  $r$  (also decreased hydrophobicity). The withdrawing effect increases the possibility of the copper being bound to the substrate, bringing the second hydroxyl group in C-2 nearer, inducing deprotonation and proton transfer to the protonated peroxide, facilitating enzyme suicide and the release of copper (0) and hydrogen peroxide. Lastly, poor tyrosinase substrates, like protocatechuic acid, protocatechuic aldehyde and 4-nitrocatechol, whose  $\delta_1$  are very high, order themselves in accordance with the values described in Table 2. Their very low values of  $k_{cat}$ ,  $\lambda_{max}$  and  $r$  can be explained by the same withdrawing effect of the group in C-4.

**Parameter  $r$**

The values of the parameter  $r$  (number of turnovers that one mol of enzyme makes before its suicide inactivation) is shown in Table 2. The values were obtained from the slopes shown in Fig. 3 and using Equation 5. From the mechanism shown in Scheme I and Equation 5, it can be concluded that the second nucleophilic attack step of the oxygen of the hydroxyl group of C-2 (controlled by  $k_{7_2}$ ) on the second copper atom in diaxial position is much faster than the deprotonation of the hydroxyl group in C-2 towards the protonated peroxide (controlled by  $k_{7_2}^i$ ). Therefore, the values of  $r$  are high. Note how  $r$  is lower in substrates with a withdrawing group than in substrates with a donating group.

#### Values of $K_m^S$

The expression  $K_m^S$  is given by Equation S15, which describes the attack constant of the oxygen of the hydroxyl group of C-1 on the copper,  $k_{7_1}$  and the binding constant of the substrate,  $k_6$ , to the enzyme ( $E_{ox}$ ), which means that its correlation with the values of  $\delta_1$  is not similar to the correlation observed between this parameter and  $k_{cat}$  or  $\lambda_{max}$ . In the case of pyrogallol, whose hydroxyl group in C-1 is partially deprotonated at pH 7.0, the value of  $K_m^S$  will be much higher than that of catechol with its protonated hydroxyl groups. However, once the enzyme binds to pyrogallol, the latter is rapidly oxidized. Note that substrates like 4-*tert*-butylcatechol (with a voluminous group in C-4) and DHPPA and DHPAA with negative charge have high  $K_m^S$  values. This implies that the catalytic efficiency ( $\lambda_{max} r / K_m^S$ ) and inactivation ( $\lambda_{max} / K_m^S$ ) are greater in substrates whose R is H (catechol),  $-\text{CH}_3$  (4-methylcatechol) or  $-\text{CH}_2\text{-CH}_3$  (4-ethylcatechol) (Table 2).

#### Proposed structural mechanism to explain suicide inactivation

Three possible mechanisms have been proposed to explain the suicide inactivation of tyrosinase: (i) an attack by the *o*-quinone product of oxidation on a sensitive group vicinal to the active site (5), (ii) a free radical attack on the active site by reactive oxygen species generated during the catalytic oxidation [7] and, more recently, (iii) the processing of a catechol as though it was a monophenol (“cresolase”-type presentation) [20]. The first two hypotheses have been rejected because the inactivation takes place even in the presence of *NADH* or *AH<sub>2</sub>*, whose presence prevents the *o*-quinone binding to the enzyme [13,21]. In addition, experiments that try to protect the enzyme from the action of free radicals were also unsuccessful [9,21]. Neither were we able to mark the enzyme in the process of suicide inactivation in experiments using [U-<sup>14</sup>C]phenol [13]. As regards the third hypothesis, which implies the presentation of a catechol in the form of a “cresolase”, the authors [20] suggested that an intermediate product is formed that can undergo deprotonation and reductive elimination; this assumes that the orientation of the phenyl ring in the enzyme-substrate complex is approximately orthogonal to the plane defined by the copper and oxygen atoms [44-46]. The experiments carried out in the present work and previously [13-15] show that: (a) the enzyme undergoes inactivation in the presence of pyrogallol (see Table 2) with a very high inactivation constant; (b) the process of suicide inactivation does not depend on pH [13], although the  $K_m^S$  apparently increases at acid pH values, and so the apparent inactivation constant decreases with pH, although the maximum apparent inactivation constant ( $\lambda_{\max}$ ) remains constant, as does  $k_{cat}$  [13].

Therefore, none of the hypotheses proposed explain the experimental data. Based on previous results, [13-15,19,22-28] and those of this work, we propose an alternative mechanism to explain the diphenolase catalytic cycle and suicide inactivation. The catalytic cycle, Step 1, begins with the  $E_m$  form non-covalently binding to S to give  $E_mS$ , perhaps forming a hydrogen bridge between the base B

(possibly a histidine) and the hydroxyl group of the substrate C-1. In Step 2, the enzyme with the help of base B withdraws the proton from the hydroxyl group of C-1 and so the substrate binds axially to the copper (by C-1) [25]. Then, the hydroxyl group of C-2 of the substrate transfers a proton to the histidine [43], separating it from the copper atom and binding diaxially with both copper atoms in Step 3. Note that the distance between the copper atoms in the  $E_m$  form is 2.9 Å. In this way, the substrate is co-planar with the copper atoms and the concerted redox reaction can occur, yielding *o*-quinone. Thus, the copper atoms change from  $Cu^{2+} Cu^{2+}$  in the *met* form to  $Cu^{1+} Cu^{1+}$  in the *deoxy* form,  $E_d$ , (Step 4). Due to the low  $K_m^{O_2}$  and the high oxygen concentration in the medium,  $E_d$  becomes  $E_{ox}$  (Step 5), with  $Cu^{2+} Cu^{2+}$  and a peroxide group co-planar with the two atoms. Next, the  $E_{ox}$  form binds another molecule from the substrate (Step 6). In this case, the base is already protonated and cannot help the substrate bind to the copper. The proton of the hydroxyl group of C-1 must be transferred to the peroxide group, which acts as a base [27,43,47]. This would be the slow step of the turnover, controlled by  $k_7$  (Step 7) [27,43,47]. The fact that the peroxide acts as a base and is involved in the proton transfer from the hydroxyl group of C-1 and C-2 is important. Note that this step of peroxide group protonation has also been proposed in [43]. The protonated peroxide draws the copper atoms in the  $E_{ox}$  form closer since its distance in the unprotonated form, 3.6 Å, is too far for the molecule of substrate to bind diaxially. However, this would be possible in the protonated  $E_{ox}$  form. With the substrate axially bound to one copper atom, there are two possibilities (Step 8): (a) the oxygen of the hydroxyl group of C-2 may attack the other copper atom which is drawn closer following protonation of the peroxide, transferring the proton to the histidine [43], binding to the substrate diaxially and co-planar with the copper atoms. In this way, the concerted redox reaction (Step 9) can occur, releasing *o*-quinone and  $E_m$ . (b) The hydroxyl group of C-2 may cede a proton

to the protonated peroxide, remaining as C-O<sup>-</sup> (Step 10). The co-planarity of the substrate ring, the oxygen of C-1 and the copper atom favour the simultaneous oxidation of the substrate to *o*-quinone and the reduction of one Cu<sup>2+</sup> atom to copper (0) through the ring, while copper (0) and hydrogen peroxide are released, and the enzyme is inactivated as a consequence (Step 11). A more detailed representation of Steps 8-11 is provided in Scheme SII (supplementary material). Note that the observation concerning the possibility of a bidentated union of the *o*-diphenol with one copper atom may also lead to suicide inactivation [48]. Axial/equatorial-type bidentated structures have also been proposed for the binding of *o*-diphenols to copper (but only one copper) and have been seen by X-ray diffraction to be co-planar [49]. However, the axial/equatorial binding to one copper atom in tyrosinase is not co-planar and so the oxidation/reduction reaction cannot take place. For this reason Steps 10 and 11 have been proposed in the mechanism of Scheme I. The inactivation mechanism is consistent with the experimental observation that 50 % of the copper is lost from the active site during catechol inactivation [21] and also with the experiments carried out [20] concerning the impossibility of reactivating the inactivated enzyme by adding Cu<sup>2+</sup>, perhaps indicating the need for a “caddie” protein [43].

The physiological significance of the suicide inactivation of tyrosinase is not clear, although it could be taken as a limitation to the action of an enzyme that generates cytotoxic products, in this case *o*-quinones [20].

## CONCLUSIONS

In this work, a kinetic study of the suicide inactivation of tyrosinase during its action on a variety of substrates has been described, and a mechanism has been proposed to explain the experimental kinetic results and to throw light on the suicide inactivation step of mushroom tyrosinase. Both processes, catalysis and inactivation, are affected by a series of factors related with the enzyme-substrate interaction. From the data obtained, it is clear that electronic, steric and hydrophobic effects play an important role in both processes. Substrates with R=H in C-4 (pyrogallol and catechol) are the best substrates for catalysis and inactivation, although the enzyme must undertake more turnovers (higher  $r$ ). Other substrates, with a large group in C-4 or with negative charges in the C-4 chain, have a steric or hydrophobic effect on both processes. Lastly, substrates with an electron-withdrawing group in C-4 (4-nitrocatechol, protocatechuic acid and protocatechuic aldehyde) show the lowest values of  $k_{cat}$  and  $\lambda_{max}$ , and so the enzyme needs to undertake fewer turnovers before being inactivated.

## ACKNOWLEDGEMENTS

This paper was partially supported by grants from the Ministerio de Educación y Ciencia (Madrid, Spain) Project BIO2006-15363 and SAF2006-07040-C02-01, from the Fundación Séneca (CARM, Murcia, Spain) Project 00672/PI/04, and from the Consejería de Educación (CARM, Murcia, Spain) BIO-BMC 06/01-0004. JLMM has a fellowship from the Ministerio de Educación y Ciencia (Madrid, Spain) Reference AP2005-4721. FGM has a fellowship from Fundación Caja Murcia (Murcia, Spain).

## REFERENCES

- 1 Sanchez-Ferrer, A., Rodriguez-Lopez, J.N., Garcia-Canovas, F. and Garcia-Carmona, F. (1995) Tyrosinase: a comprehensive review of its mechanism. *Biochim. Biophys. Acta* **1247**, 1-11.
- 2 Halaouli, S., Asther, M., Sigoillot, J.C., Hamdi, M. and Lomascolo, A. (2006) Fungal tyrosinases: new prospects in molecular characteristics, bioengineering and biotechnological applications. *J. Appl. Microbiol.* **100**, 219-232.
- 3 Nelson, J.M. and Dawson, C.R. (1944) Tyrosinase. *Adv. Enzymol.* **4**, 99-152.
- 4 Asimov, I. and Dawson, C.R. (1950) On the reaction inactivation of tyrosinase during the aerobic oxidation of catechol. *J. Am. Chem. Soc.* **72**, 820-828.
- 5 Ingraham, L.L., Corse, J. and Makower, B. (1952) Enzymatic browning of fruits .3. kinetics of the reaction inactivation of polyphenol oxidase. *J. Am. Chem. Soc.* **74**, 2623-2626.
- 6 Tomita, Y. and Seiji, M. (1977) Inactivation mechanism of tyrosinase in mouse melanoma. *J. Dermatol.* **4**, 245-249.
- 7 Seiji, M., Sasaki, M. and Tomita, Y. (1978) Nature of tyrosinase inactivation in melanosomes. *Tohoku J. Exp. Med.* **125**, 233-245.
- 8 Tomita, Y., Hariu, A., Mizuno, C. and Seiji, M. (1980) Inactivation of tyrosinase by dopa. *J. Invest. Dermatol.* **75**, 379-382.

- 9 Lerch, K. (1983) Neurospora tyrosinase: structural, spectroscopic and catalytic properties. *Mol. Cell. Biochem.* **52**, 125-138.
- 10 Zhong, J.Y. and Groutas, W.C. (2004) Recent developments in the design of mechanism-based and alternate substrate inhibitors of serine proteases. *Curr. Top. Med. Chem.* **4**, 1203-1216.
- 11 Ghanbari, F., Rowland-Yeo, K., Bloomer, J.C., Clarke, S.E., Lennard, M.S., Tucker, G.T. and Rostami-Hodjegan, A. (2006) A critical evaluation of the experimental design of studies of mechanism based enzyme inhibition, with implications for in vitro-in vivo extrapolation. *Curr. Drug Metab.* **7**, 315-334.
- 12 Silverman, R.B. (1995) Mechanism-based enzyme inactivators. *Meth. Enzymol.* **249**, 240-283.
- 13 Garcia-Canovas, F., Tudela, J., Martinez-Madrid, C., Varon, R., Garcia-Carmona, F. and Lozano J.A. (1987) Kinetic study on the suicide inactivation of tyrosinase induced by catechol. *Biochim. Biophys. Acta* **912**, 417-423.
- 14 Tudela, J., Garcia-Canovas, F., Varon, R., Jimenez, M., Garcia-Carmona, F. and Lozano J.A. (1987) Kinetic characterization of dopamine as a suicide substrate of tyrosinase. *J. Enzyme Inhibition* **2**, 47-56.
- 15 Tudela, J., Garcia-Canovas, F., Varon, R., Jimenez, M., Garcia-Carmona, F. and Lozano J.A. (1988) Kinetic study in the transient phase of the suicide inactivation of frog epidermis tyrosinase. *Biophys. Chem.* **30**, 303-310.

- 16 Arnao, M.B., Acosta, M., del Rio, J.A., Varon, R. and Garcia-Canovas, F. (1990) A kinetic-study on the suicide inactivation of peroxidase by hydrogen-peroxide. *Biochim. Biophys. Acta* **1041**, 43-47.
- 17 Hiner, A., Hernandez-Ruiz, J., Arnao, M.B., Garcia-Canovas, F. and Acosta, M. (1996) A comparative study of the purity, enzyme activity, and inactivation by hydrogen peroxide of commercially available horseradish peroxidase isoenzymes A and C. *Biotechnology and Bioengineering* **50**, 655-662.
- 18 Escribano, J., Tudela, J., Garcia-Carmona, F. and Garcia-Canovas, F. (1989) A kinetic-study of the suicide inactivation of an enzyme measured through coupling reactions: application to the suicide inactivation of tyrosinase. *Biochem. J.* **262**, 597-603.
- 19 Garcia-Canovas, F., Tudela, J., Varon, R. and Vazquez, A.M. (1989) Experimental methods for kinetic study of suicide substrates. *J. Enzyme Inhibition* **3**, 81-90.
- 20 Land, E.J., Ramsden, C.A. and Riley, P.A. (2007) The mechanism of suicide-inactivation of tyrosinase: A substrate structure investigation. *Tohoku J. Exp. Med.* **212**, 341-348.
- 21 Dietler, C. and Lerch, K. (1982) in *Oxidases and Related Redox Systems* (King, T.E., Mason, H.S., and Morrison, M., ed), pp. 305-317, Pergamon Press, New York.
- 22 Espin, J.C., Varon, R., Fenoll, L.G., Gilarbert, M.A., Garcia-Ruiz, P.A., Tudela, J. and Garcia-Canovas, F., (2000) Kinetic characterization of the substrate specificity and mechanism of mushroom tyrosinase. *Eur. J. Biochem.* **267**, 1270-1279.

- 23 Fenoll, L.G., Rodriguez-Lopez, J.N., Varon, R., Garcia-Ruiz, P.A., Garcia-Canovas, F. and Tudela, J. (2002) Kinetic characterisation of the reaction mechanism of mushroom tyrosinase on tyramine/dopamine and L-tyrosine methyl ester/L-dopa methyl ester. *Int. J. Biochem. Cell Biol.* **34**, 1594-1607.
- 24 Fenoll, L.G., Rodriguez-Lopez, J.N., Garcia-Sevilla, F., Garcia-Ruiz, P.A., Varon, R., Garcia-Canovas, F. and Tudela, J. (2001) Analysis and interpretation of the action mechanism of mushroom tyrosinase on monophenols and diphenols generating highly unstable *o*-quinones. *Biochim. Biophys. Acta* **1548**, 1-22.
- 25 Rodriguez-Lopez, J.N., Fenoll, L.G., Garcia-Ruiz, P.A., Varon, R., Tudela, J., Thorneley, R.N. and Garcia-Canovas, F. (2000) Stopped-flow and steady-state study of the diphenolase activity of mushroom tyrosinase. *Biochemistry* **39**, 10497-10506.
- 26 Ros, J.R., Rodriguez-Lopez, J.N. and Garcia-Canovas, F. (1994) Tyrosinase kinetic analysis of the transient phase and the steady-state. *Biochim. Biophys. Acta* **1204**, 33-42.
- 27 Fenoll, L.G., Penalver, M.J., Rodriguez-Lopez, J.N., Garcia-Ruiz, P.A., Garcia-Canovas, F. and Tudela, J. (2004) Deuterium isotope effect on the oxidation of monophenols and *o*-diphenols by tyrosinase. *Biochem. J.* **380**, 643-650.
- 28 Rodriguez-Lopez, J.N., Fenoll, L.G., Penalver, M.J., Garcia-Ruiz, P.A., Varon, R., Martinez-Ortiz, F., Garcia-Canovas, F. and Tudela, J. (2001) Tyrosinase action on monophenols: evidence for direct enzymatic release of *o*-diphenol. *Biochim. Biophys. Acta* **1548**, 238-256.

- 29 Garcia Molina, F., Munoz, J.L., Varon, R., Rodriguez Lopez, J.N., Garcia Canovas, F. and Tudela, J. (2007) An approximate analytical solution to the lag period of monophenolase activity of tyrosinase. *Int. J. Biochem. Cell. Biol.* **39**, 238-252.
- 30 Garcia-Molina, F., Munoz, J.L., Varon, R., Rodriguez-Lopez, J.N., Garcia-Canovas, F. and Tudela, J. (2007) A review on spectrophotometric methods for measuring the monophenolase and diphenolase activities of tyrosinase. *J. Agric. Food Chem.* **55**, 9739-9749.
- 31 Rodriguez-Lopez, J.N., Ros, J.R., Varon, R. and Garcia-Canovas, F. (1993) Oxygen Michaelis constants for tyrosinase. *Biochem. J.* **293**, 859-866.
- 32 Garcia-Carmona, F., Garcia-Canovas, F., Iborra, J.L. and Lozano, J.A. (1982) Kinetic study of the pathway of melanization between L-dopa and dopachrome. *Biochim. Biophys. Acta* **717**, 124-131.
- 33 Garcia-Canovas, F., Garcia-Carmona, F., Vera-Sanchez, J., Iborra, J.L. and Lozano, J.A. (1982) The role of pH in the melanin biosynthesis pathway. *J. Biol. Chem.* **257**, 8738-8744.
- 34 Munoz, J.L., Garcia-Molina, F., Varon, R., Rodriguez-Lopez, J.N., Garcia-Canovas, F. and Tudela, J. (2006) Calculating molar absorptivities for quinones: application to the measurement of tyrosinase activity. *Anal. Biochem.* **351**, 128-138.
- 35 Lowry, O.H., Rosebrough, N.J., Farr, A.L. and Randall, R.J. (1951) Protein measurement with the Folin phenol reagent. *J. Biol. Chem.* **193**, 265-275.

- 36 Jandel Scientific. Sigma Plot 9.0 for Windows™; Jandel Scientific: Core Madera 2006.
- 37 Fenoll, L.G., Rodriguez-Lopez, J.N., Garcia-Molina, F., Garcia-Canovas, F. and Tudela, J. (2002) Michaelis constants of mushroom tyrosinase with respect to oxygen in the presence of monophenols and diphenols. *Int. J. Biochem. Cell Biol.* **34**, 332-336.
- 38 Walsh, C.T. (1984) Suicide substrates, mechanism-based enzyme inactivators: recent developments. *Annu. Rev. Biochem.* **53**, 493-535.
- 39 Haghbeen, K., Saboury, A.A. and Karbassi, F. (2004) Substrate share in the suicide inactivation of mushroom tyrosinase. *Biochim. Biophys. Acta* **1675**, 139-146.
- 40 Garcia-Molina, F., Hiner, A.N., Fenoll, L.G., Rodriguez-Lopez, J.N., Garcia-Canovas, F. and Tudela, J. (2005) Mushroom tyrosinase: Catalase activity, inhibition, and suicide inactivation. *J. Agric. Food Chem.* **53**, 3702-3709.
- 41 Espin, J.C, Morales, M., Varon, R., Tudela, J. and Garcia-Canovas, F. (1995) A continuous spectrophotometric method for determining the monophenolase and diphenolase activities of apple polyphenol oxidase. *Anal. Biochem.* **231**, 237-246.
- 42 Espin, J.C, Garcia-Ruiz, P.A., Tudela, J., Varon, R. and Garcia-Canovas, F. (1998) Monophenolase and diphenolase reaction mechanisms of apple and pear polyphenol oxidases. *J. Agric. Food Chem.* **46**, 2968-2975.

- 43 Matoba, Y., Kumagai, T., Yamamoto, A., Yoshitsu, H. and Sugiyama, M (2006) Crystallographic evidence that the dinuclear copper center of tyrosinase is flexible during catalysis. *J. Biol. Chem.* **281**, 8981-8990.
- 44 Decker, H., Schweikardt, T. and Tuczec, F. (2006) The first crystal structure of tyrosinase: all questions answered?. *Angew. Chem. Int. Ed.* **45**, 4546-4550.
- 45 Van Gastel, M., Bubacco, L., Groenen, E.J.J., Vijgenboom, E. and Canters, G.W. (2000) EPR study of the dinuclear active copper site of tyrosinase from *Streptomyces antibioticus*. *FEBS Letters* **474**, 228-232.
- 46 Bubacco, L., Van Gastel, M., Groenen, E.J.J., Vijgenboom, E. and Canters, G.W. (2003) Spectroscopic characterization of the electronic changes in the active site of *Streptomyces antibioticus* tyrosinase upon binding of transition state analogue inhibitors. *J. Biol. Chem.* **278**, 7381-7389.
47. Peñalver, M.J., Rodriguez-Lopez, J.N., Garcia-Ruiz, P.A., Garcia-Canovas, F., and Tudela, J. (2003) Solvent deuterium isotope effect on the oxidation of the *o*-diphenols by tyrosinase. *Biochim. Biophys. Acta* **1650**, 128-135.
- 48 Decker, H., Schweikardt, T., Nillius, Dd., Salzbrunn, U., Jaenicke, E. and Tuczec, F. (2007) Similar enzyme activation and catalysis in hemocyanins and tyrosinases. *Gene* **398**, 183-191.
- 49 Speier, G., Tisza, S., Tyeklar, Z., Lange, C.W. and Pierpont, C.G. (1994) Coligand-dependent shifts in charge-distribution for copper-complexes containing 3,5-di-*tert*-butylcatecholate and 3,5-di-*tert*-butylsemiquinonate ligands. *Inorg. Chem.* **33**, 2041-2045.

## FIGURES AND SCHEMES LEGENDS

FIGURE 1. **Experimental recordings of the disappearance of  $AH_2$  in the suicide inactivation of tyrosinase by pyrogallol and curves corrected after applying the data analysis.** Conditions were 30 mM phosphate buffer pH 7.0,  $[AH_2]_0$  0.2 mM,  $[SOD]_0$  1.2  $\mu$ M,  $[O_2]_0$  0.26 mM and  $[Pyrogallol]_0$  1.5 mM. The enzyme concentrations (nM) were: (a) 0.12 and (c) 0.30. Curves (b) and (d) are the corrected recordings from (a) and (c), respectively.

FIGURE 2. **Corrected recordings of the disappearance of  $AH_2$  in the suicide inactivation of tyrosinase by pyrogallol for different enzyme concentrations.** Conditions were 30 mM phosphate buffer pH 7.0,  $[SOD]_0$  1.2  $\mu$ M,  $[AH_2]_0$  0.2 mM,  $[Pyrogallol]_0$  1.5 mM, while enzyme concentrations (nM) were (a) 0.06, (b) 0.12, (c) 0.17, (d) 0.24, (e) 0.3, (f) 0.35 and (g) 0.39. Inset. Corresponding values of  $[Q]_\infty$  and  $\lambda$  for different concentrations of tyrosinase.

FIGURE 3. **Representations of the values of  $[Q]_\infty$  vs. enzyme concentration for the different substrates studied.** Experimental conditions were 30 mM phosphate buffer pH 7.0, 25 °C. Catechol, 4-methylcatechol, 4-ethylcatechol, 4-chlorocatechol, 4-*tert*-butyl-catechol, DHPPA, DHPAA, protocatechuic acid, protocatechuic aldehyde and 4-nitrocatechol were recorded from the disappearance of  $NADH$  with  $[NADH]_0$  0.2 mM for every substrate; Pyrogallol and gallic acid were recorded from the disappearance of  $AH_2$  and gallic acid methyl ester was recorded measuring oxygen consumption, with  $AH_2$  and  $SOD$  ( $[AH_2]_0$  0.2 mM,  $[SOD]_0$  1.2  $\mu$ M for every substrate). Substrates (mM):  $[4\text{-}tert\text{-Butylcatechol}]_0$  2,  $[DHPPA]_0$  3,  $[DHPAA]_0$  1.5,  $[\text{gallic acid methyl ester}]_0$  0.3,  $[\text{gallic acid}]_0$  0.1,  $[\text{protocatechuic acid}]_0$  0.5,

[protocatechuic aldehyde]<sub>0</sub> 0.1, [4-nitrocatechol]<sub>0</sub> 0.1, [Pyrogallol]<sub>0</sub> 1.5, [catechol]<sub>0</sub> 0.3, [4-chlorocatechol]<sub>0</sub> 0.15, [4-methylcatechol]<sub>0</sub> 0.6 and [4-ethylcatechol]<sub>0</sub> 0.15. In every substrates, (—) Linear regression fitting of the experimental data points.

**FIGURE 4. Corrected recordings of the disappearance of  $AH_2$  in the suicide inactivation of tyrosinase by pyrogallol for different substrate concentrations.**

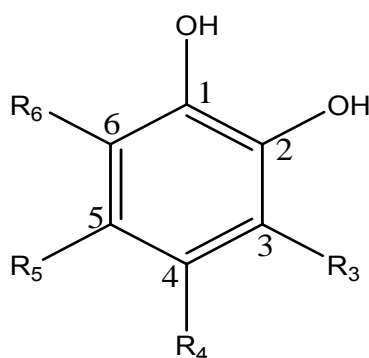
Conditions were 30 mM phosphate buffer pH 7.0,  $[AH_2]_0$  0.2 mM,  $[SOD]_0$  1.2  $\mu$ M,  $[E]_0$  0.23 nM, while substrate concentrations (mM) were (a) 1, (b) 1.5, (c) 2, (d) 2.5, (e) 3, (f) 4 and (g) 5. Inset. Corresponding values of  $\lambda$  for different pyrogallol concentrations.

**FIGURE 5. Representation of the values of the inactivation constant  $\lambda$  vs.  $[S]_0$  for the different substrates studied.** Conditions were 30 mM phosphate buffer pH 7.0, 25 °C. 4-*tert*-butyl-catechol, DHPPA, DHPAA, were recorded from the disappearance of *NADH* with  $[NADH]_0$  0.2 mM for every substrate and Pyrogallol was recorded from the disappearance of  $AH_2$ , with *SOD* ( $[AH_2]_0$  0.2 mM,  $[SOD]_0$  1.2  $\mu$ M). (linear tracings) Non-linear regression fitting to Equation 6 of the data analysis. Enzyme concentrations (nM) were: Pyrogallol (0.23), 4-*tert*-butylcatechol (0.09), DHPPA (0.09) and DHPAA (0.09).

**Scheme I. Structural mechanism proposed to explain the diphenolase cycle and suicide inactivation of tyrosinase.** *Diphenolase cycle:*  $E_m$ , mettyrosinase;  $E_mS$ , interaction between  $E_m$  and S;  $(E_m-S)_1$ , axial nucleophilic attack complex from OH of C-1 to  $E_m$ ;  $(E_m-S)_2$ , diaxial binding complex of S with  $E_m$ ;  $E_d$ , deoxytyrosinase;  $E_{ox}$ , oxytyrosinase;  $E_{ox}S$ , interaction complex between  $E_{ox}$  with S;  $(E_{ox}-S)_1$ , axial binding

complex of protonated S with  $E_{ox}$ ;  $(E_{ox}-S)_2$ , diaxial binding complex of S with  $E_{ox}$ . *Suicide inactivation*:  $(E_{ox}-S)_3$ , Axial binding complex of deprotonated S with  $E_{ox}$ ;  $E_i$ , inactive enzyme.

Stage 2(a) POST-PRINT

Table 1. *o*-Diphenol structures used in this work.

<i>o</i> -Diphenol	R <sub>3</sub>	R <sub>4</sub>	R <sub>5</sub>	R <sub>6</sub>
Pyrogallol	H	H	H	OH
Catechol	H	H	H	H
4-Chlorocatechol	H	-Cl	H	H
4-Methylcatechol	H	-CH <sub>3</sub>	H	H
4-Ethylcatechol	H	-CH <sub>2</sub> -CH <sub>3</sub>	H	H
4- <i>tert</i> -Butylcatechol	H	-C-(CH <sub>3</sub> ) <sub>3</sub>	H	H
DHPPA	H	-(CH <sub>2</sub> ) <sub>2</sub> -COOH	H	H
DHPAA	H	-CH <sub>2</sub> -COOH	H	H
Gallic acid methyl ester	H	-COOCH <sub>3</sub>	H	OH
Gallic acid	H	-COOH	H	OH
Protocatechuic acid	H	-COOH	H	H
Protocatechuic aldehyde	H	-CHO	H	H
4-Nitrocatechol	H	-NO <sub>2</sub>	H	H

**Table 2. Kinetic constants which characterize the suicide inactivation of tyrosinase by different substrates and values of the chemical shifts of the different suicide substrates of tyrosinase obtained by  $^{13}\text{C}$ -NMR for the C-1 and C-2 carbons at pH 7.0.**

o-Diphenol	$\lambda_{\max} \times 10^3$ ( $\text{s}^{-1}$ )	$r = k_{\text{cat}} / \lambda_{\max}$	$k_{\text{cat}}$ ( $\text{s}^{-1}$ )	$K_m^S$ (mM)	$K_m^{O_2}$ (mM)	$\delta_1^7$ (p.p.m.)	$\delta_2^7$ (p.p.m.)
Pyrogallol	12.01 $\pm$ 0.31	122093 $\pm$ 2740	1280.3 $\pm$ 47.1	1.96 $\pm$ 0.03	55.6 $\pm$ 2.81	135.19	148.22
Catechol	8.92 $\pm$ 0.27	99994 $\pm$ 1604	874.1 $\pm$ 30.2	0.16 $\pm$ 0.01	38.0 $\pm$ 2.61	146.59	146.59
4-Chlorocatechol	8.54 $\pm$ 0.25	99356 $\pm$ 1788	859.2 $\pm$ 28.3	0.60 $\pm$ 0.03	37.3 $\pm$ 1.62	145.04	147.35
4-Methylcatechol	8.21 $\pm$ 0.25	98366 $\pm$ 1377	842.1 $\pm$ 26.1	0.10 $\pm$ 0.01	36.6 $\pm$ 2.70	144.06	146.43
4-Ethylcatechol	7.95 $\pm$ 0.23	97562 $\pm$ 1951	802.3 $\pm$ 26.1	0.17 $\pm$ 0.01	34.8 $\pm$ 2.63	143.99	146.27
4- <i>tert</i> -Butylcatechol	7.28 $\pm$ 0.28	88788 $\pm$ 1864	640.1 $\pm$ 28.1	1.45 $\pm$ 0.12	27.8 $\pm$ 2.52	144.09	146.24
DHPPA	6.93 $\pm$ 0.27	87646 $\pm$ 1315	607.2 $\pm$ 25.1	0.70 $\pm$ 0.09	26.4 $\pm$ 2.13	144.96	146.43
DHPAA	6.89 $\pm$ 0.37	62838 $\pm$ 1187	433.1 $\pm$ 25.9	1.30 $\pm$ 0.10	18.8 $\pm$ 1.31	144.61	146.51
Gallic acid methyl ester	1.70 $\pm$ 0.09	47444 $\pm$ 501	80.2 $\pm$ 3.9	0.12 $\pm$ 0.01	3.41 $\pm$ 0.11	141.42	147.34
Gallic acid	1.57 $\pm$ 0.07	18666 $\pm$ 466	28.2 $\pm$ 0.9	0.18 $\pm$ 0.01	1.12 $\pm$ 0.11	140.64	147.29
Protocatechuic acid	0.85 $\pm$ 0.03	10186 $\pm$ 224	8.1 $\pm$ 0.3	0.07 $\pm$ 0.01	0.34 $\pm$ 0.02	150.00	146.04
Protocatechuic aldehyde	0.61 $\pm$ 0.02	2554 $\pm$ 40	1.5 $\pm$ 0.1	0.15 $\pm$ 0.02	0.06 $\pm$ 0.01	155.28	146.71
4-Nitrocatechol	0.45 $\pm$ 0.02	2254 $\pm$ 41	0.9 $\pm$ 0.1	0.10 $\pm$ 0.01	0.04 $\pm$ 0.01	155.87	148.07

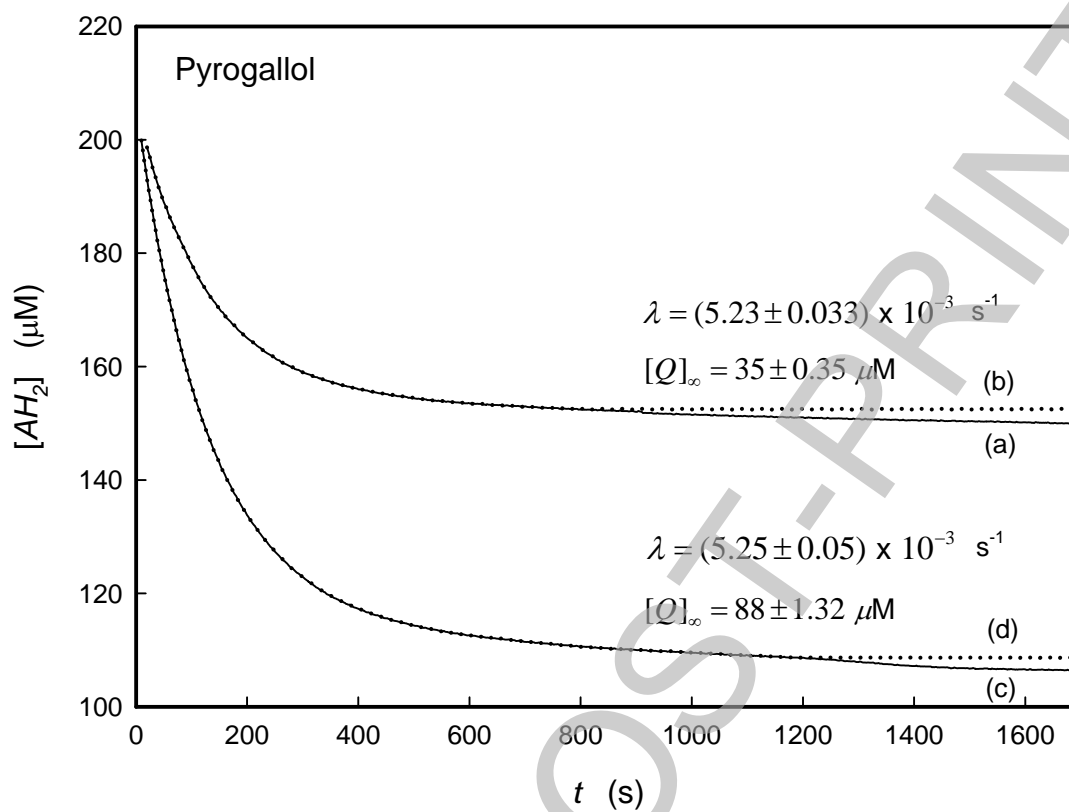


Fig. 1

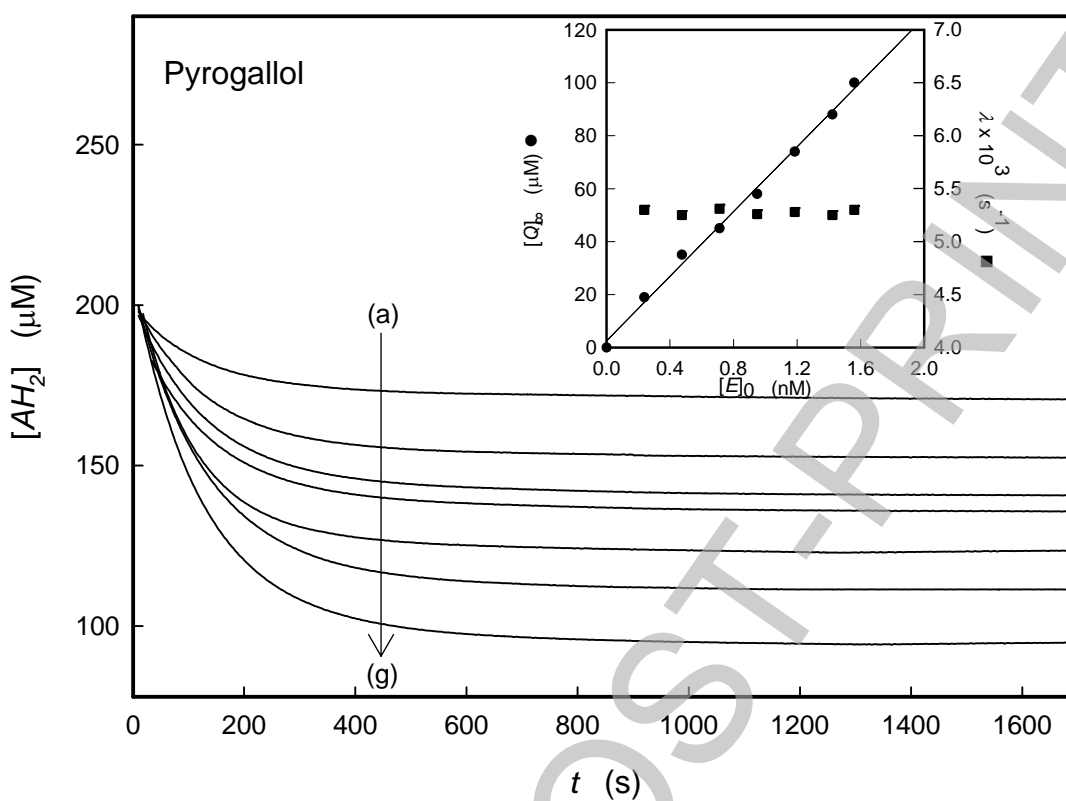


Fig. 2

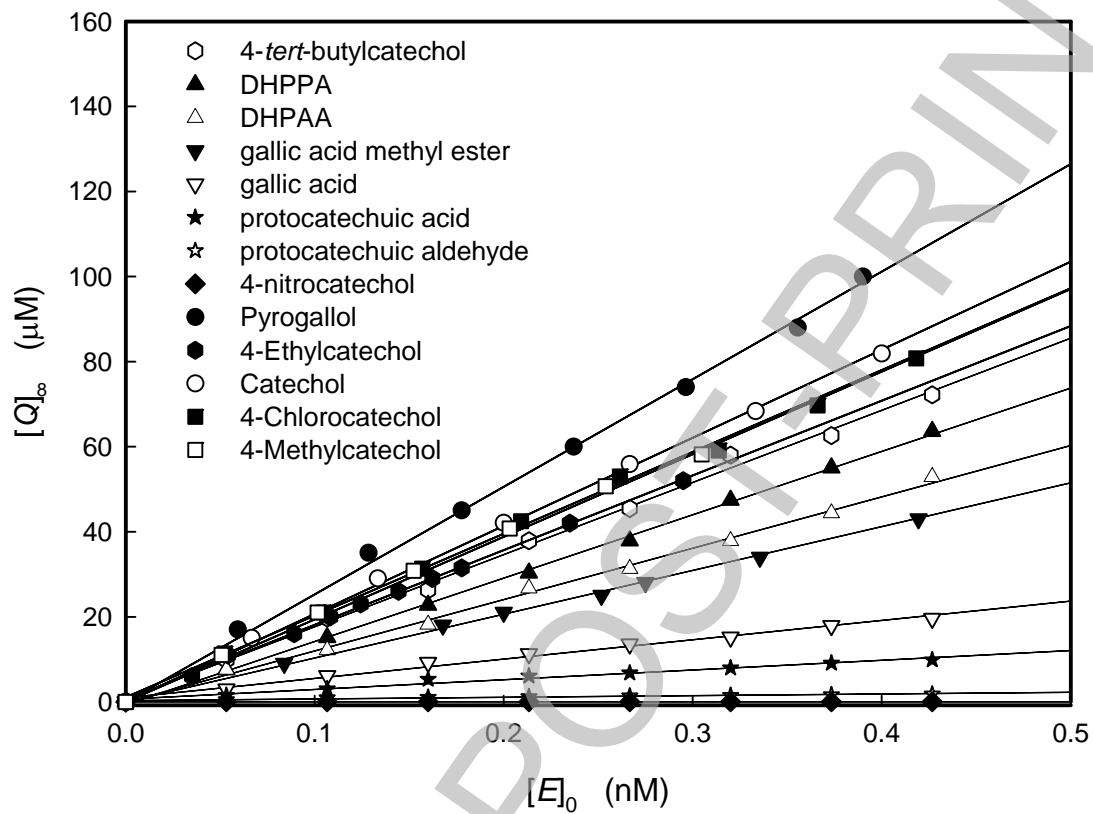


Fig. 3

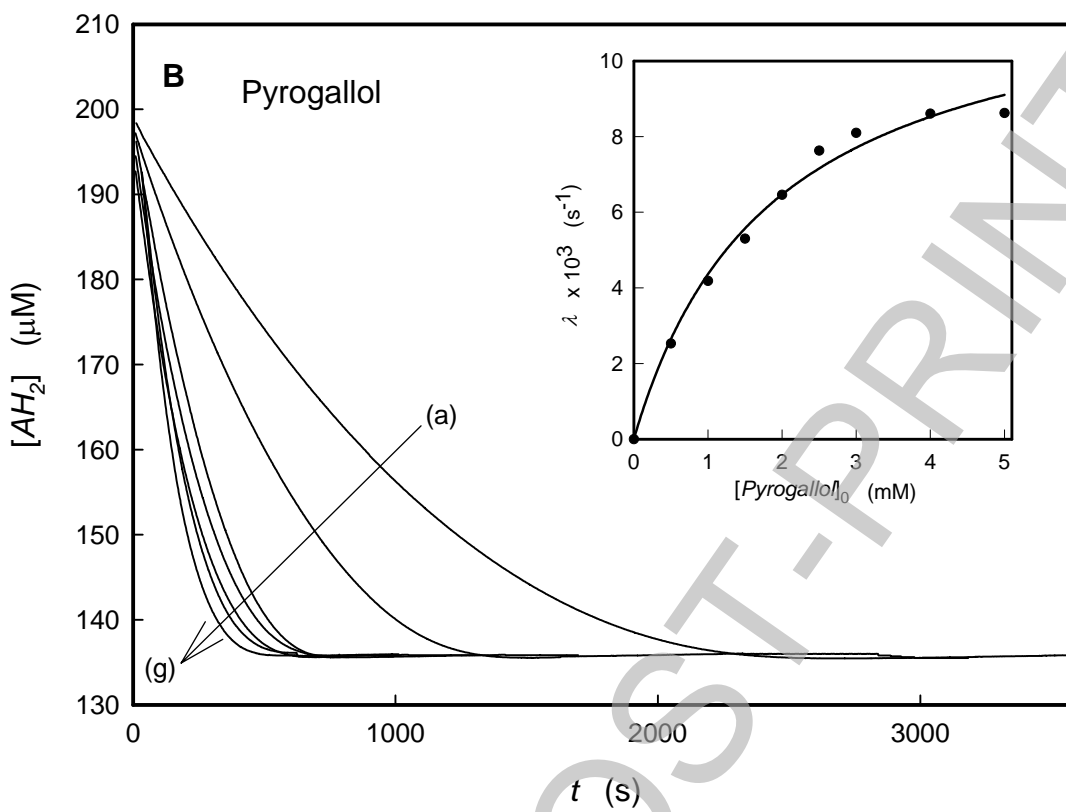


Fig. 4

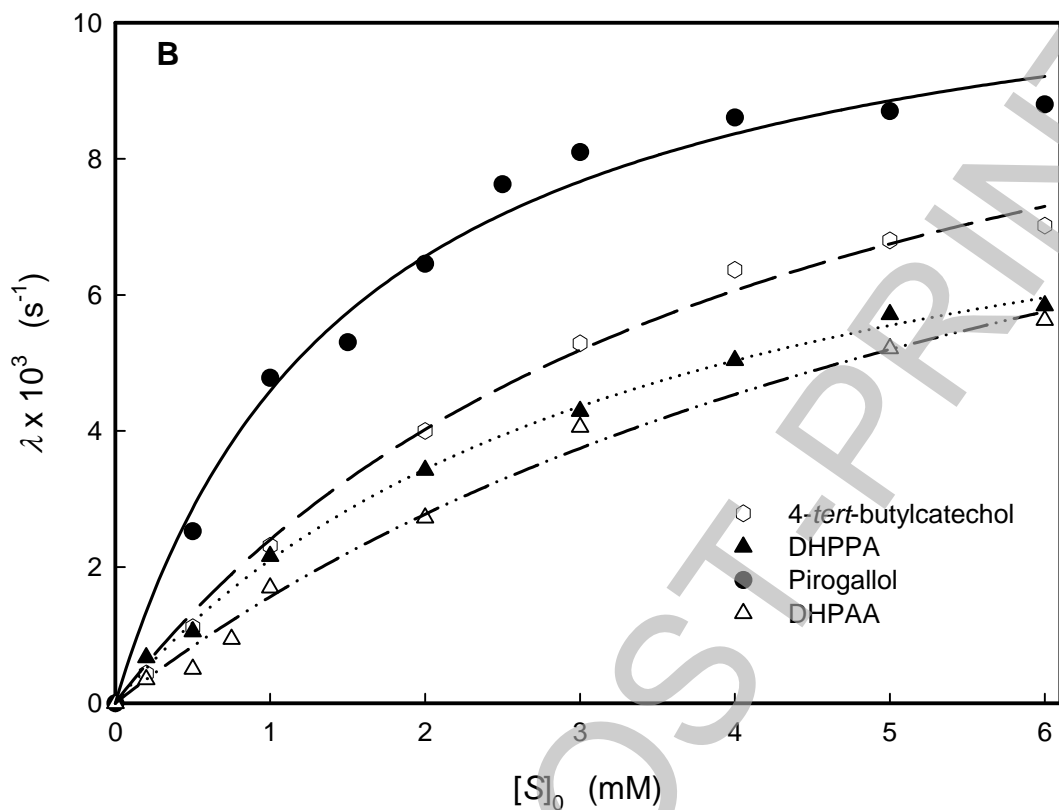


Fig. 5

